


CHARLES UNIVERSITY
Faculty of Pharmacy
in Hradec Králové

Effect of Glucosyl Sphingosine on the *stratum corneum* Permeability

Hradec Králové 2020 **Omar Mahrous Farid Bataalla**

Statement of originality

I declare that this diploma thesis is my own personal work and that I worked on it on my own. All literature and other resources that I used are listed in the references list and are properly cited.

Hradec Králové 2020 Omar Mahrous Farid Bataalla

Acknowledgments

Foremost, I would like to express my deepest appreciation to my supervisor PharmDr. Andrej Kováčik, Ph.D. for his guidance throughout my thesis. His patience and immense knowledge made this project a success. I would also like to thank to my consultant Dr. Georgios Paraskevopoulos, PhD., Mgr. Anna Nováčková, and other members of *Skin Barrier Research Group*. To my friends, thank you for your prayers and kind words. I am also thankful to the Czech Science Foundation (GAČR 19-09135J) and Charles University (SVV 260547).

Table of contents

Abstract

Glucosyl sphingosine (GSP) belongs to a large lysolipid subclass of sphingolipids, which is formed from ceramide (Cer) precursors by its hydrolysis. Patients with some skin diseases, such as atopic dermatitis, have lower amounts of barrier Cer in comparison to a healthy skin. As a result, they have higher quantity of GSP with low moisture content due to impaired barrier function. The aim of my work was to investigate the effect of GSP on skin permeability (in this thesis, the uppermost epidermal layer, the stratum corneum, was used) by using four permeability markers, trans-epidermal water loss (TEWL), electrical impedance, flux of theophylline and flux of indomethacin. The electrical impedance showed higher permeability to ions in tissues with GSP (statistically significant) in comparison to the controls. An addition of GSP also increased the permeability to water, small polar molecules and large lipophilic molecules (both statistically insignificant). I also investigated the role of GSP on the lipid chain order and microstructure of SC (studied by infrared spectroscopy). After the application of GSP, the lipid chain disorder partially increased (shift to higher wavenumbers). The general idea of this study was to confirm/disprove the effect of lysolipids on the skin permeability. The results could be useful for further study of human skin pathophysiology*, e.g.,* Gaucher disease or atopic dermatitis.

Abstrakt

Glukosyl-sfingosin (GSP) je součástí podtřídy lysolipidů a patří do rodiny sfingolipidů, které jsou tvořeny pomocí hydrolytických reakcí z ceramidových prekurzorů. Pacienti trpící kožními nemocemi, jako např. atopickou dermatitidou, mají nižší hladiny bariérových ceramidů v porovnání se zdravými jedinci. Zároveň u těchto nemocných byly nalezeny zvýšené hladiny GSP a nižší hydratace pokožky, s čím souvisí snížená (poškozená) bariérová funkce kůže. Cílem této práce bylo hodnotit význam GSP na propustnost kůže (v této práce jsme použili nejsvrchnější kožní vrstvu, *stratum corneum*, SC) pomocí různých markerů propustnosti – transmembránová ztráta vody (TEWL), elektrická impedance, flux teofylinu a flux indometacinu. Získané hodnoty elektrické impedance naznačují, že membrány po aplikaci GSP jsou více propustné (statisticky významné) pro ionty ve srovnání s kontrolou. Přídavek GSP na rohovou vrstvu zvyšuje její propustnost pro vodu, malé polární molekuly a větší lipofilní molekuly. Dále byl hodnocen vliv GSP na uspořádání lipidů a mikrostrukturu SC, a to pomocí infračervené spektroskopie. Po aplikaci GSP na SC bylo částečně pozorováno horší uspořádání lipidů SC (posun vlnočtů symetrických vibrací do vyšších vlnočtů). Základní myšlenkou této práce bylo potvrdit/vyvrátit vliv lysolipidů na propustnost kůže (bariérovou funkci kůže). Výsledky této diplomové práce by mohly posloužit dalšímu hodnocení patofyziologie lidské kůže, např. studium Gaucherovy nemoci či atopické dermatitidy.

1. Introduction

1.1. Human skin function

Human skin is considered as the largest organ of the human body. It protects us from ultraviolet radiation by a pigment found in the skin called melanin. Skin also protects our body from infections (bacteria, viruses), it acts as a waterproof preventing our body from dehydration and skin also regulates body temperature. Skin also acts as a reservoir for vitamin D synthesis.[1-5]

1.2. Human skin composition

Human skin is composed of three basic layers, *i.e.,* the epidermis, dermis, and the innermost layer, known as hypodermis (**Figure 1**).

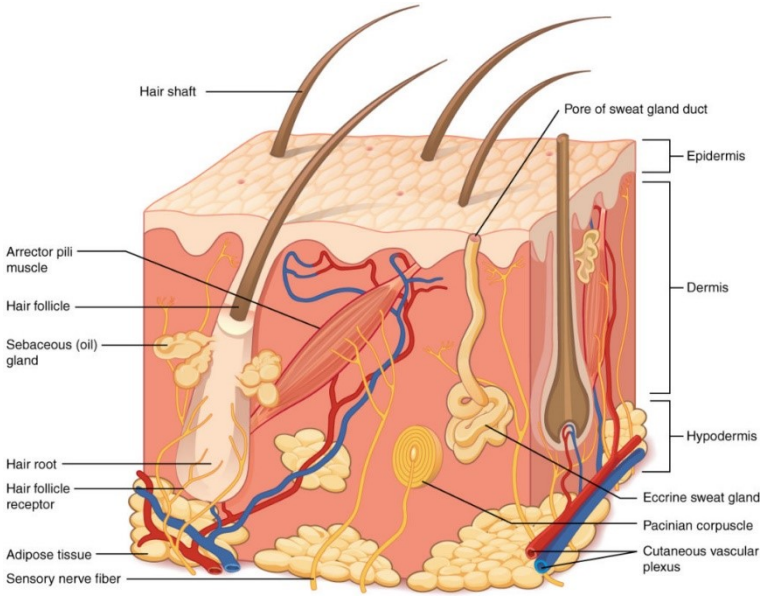

***Figure 1**. Structure of human skin, i.e., skin layers (epidermis, dermis, and hypodermis).*[6]

Hypodermis is also known as subcutaneous fatty layer; it is located below the dermis and it consists of collagen fibres, which maintain the fat cells (adipocytes containing different types of vacuoles filled with triglycerides), which are joined with blood vessels. The main function of hypodermis is to protect the human body against mechanical agents, it also plays a role as a reservoir of fat (energy for some metabolic processes).[7]

Dermis is located under the epidermis; it is 20 to 30 times wider than epidermis and it consists of blood capillaries, sweat glands, hair follicles, sebaceous glands, sensory nerve endings, etc. These skin derivatives are shown in **Figure 1**. Dermis consists of two layers known as papillary layer, which contains phagocytes engulfing bacteria and reticular layer, which contain elastin and collagen fibres. The elastin and collagen fibres are necessary for the typical skin properties*, i.e.,* the elasticity and plasticity. The amount of these structures in the dermis depends on many factors, *e.g.,* an age of human.[4, 5]

Epidermis is the outermost layer of the skin. It contains cells called keratinocytes. It consists of five layers and they are as follows: *stratum basale, stratum spinosum, stratum granulosum, stratum lucidum, and the outermost layer, stratum corneum* (**Figure 2**). According to the presence of the *stratum corneum*, epidermis can be divided into dead part of epidermis (formed practically by *stratum corneum*) and living part, called as viable epidermis. [4]

Stratum basale is innermost layer; it is where keratinocytes are formed and it also contains melanocytes (melanin pigments are formed), Langerhans cells (dendritic cells) and Merkel cells (stimulated by sensory nerves).[5]

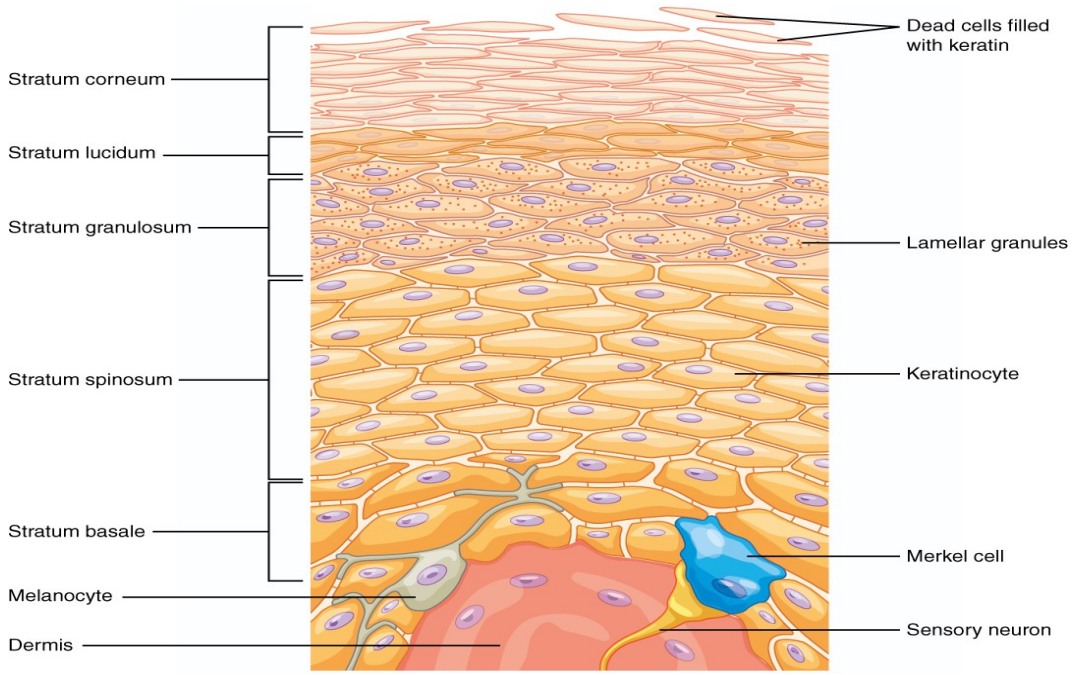

Figure 2*. Structure of human epidermis, i.e., stratum basale, stratum spinosum, stratum granulosum, stratum lucidum, and outermost layer, the stratum corneum.*[6]

Stratum spinosum is localized between *stratum basale* and *stratum granulosum*. It consists of 8-10 layers of keratinocytes; the keratinocytes produce keratin. It also contains Langerhans cells, which immerse bacteria and foreign particles. It liberates glycoprotein, which helps the skin waterproof.[4, 5]

Stratum granulosum consists of approximately five layers of keratinocytes with granules liberating lipids. These lipids in upper layers prevent our body from water loss. The cells also produce significant amount of keratin and keratohyallin.[8, 9]

Stratum lucidum is localized between *stratum corneum* and *stratum granulosum*; it consists of five layers of keratinocytes. This layer was found on thick skin such as the hands and feet. They contain some proteins, derived from keratohyallin.[9]

Statum corneum (SC; **Figure 2**) is the outermost epidermal layer; it acts as a skin barrier and it consists of approximately 15-30 layers of dead keratinocytes, well known as **corneocytes**. SC protects our body from dehydration and infections such as bacteria or viruses. This layer is crucial for life on the terrestrial land. The skin barrier is localized in this layer.[5]

SC is composed of dead flat cells (keratinocytes) = **corneocytes**. These cells are filled with proteins (mainly keratin and filaggrin = filament aggregating protein); they do not contain any compartments, such as nuclei, etc. They are enclosed into the **lipid matrix** (see below) which is a unique lipidic mixture, see below. The thickness of corneocytes is approximately 0.3 μm and they are 30 μm in diameter.[5, 9]

The SC lipid matrix consists of **free fatty acids**, **cholesterol** and **ceramides** (Cer)[3] as shown in **Figure 3.** These skin lipids occur there in the molar ratio of 1:1:1. [3] This molar ratio is crucial for the proper barrier function. Cer together with other lipids form lipid lamellae. In the healthy SC, two lamellar organizations have been found. The first is known as long periodicity phase (with length of lamellae approximately 12-13 nm)[10] and the second is short periodicity phase, where the lipids form lamellae with 5-6 nm periodicity.[11] The long periodicity phase (known under acronym LPP) was identified by electron microscopy [12]and by X-ray diffraction.[13] In addition, a phase of separated cholesterol (with approximately 3.4 nm periodicity[14]) was found in the healthy SC. In total, three phases occur in SC: short periodicity phase (SPP), LPP, and separated cholesterol.

Most of the **free fatty acids** are unbranched and saturated; unsaturated are present only in small amount and in patients with atopic dermatitis (AD)[15] (their amount is higher due to filaggrin deficiency; they consist of 14-34 carbons. The number of carbons in the healthy human barrier fatty acids ranges between 16 and 24. The most abundant free fatty acids in SC is lignoceric (C24) and cerotic acid(C24).[16-18]

Cholesterol is the main sterol type. Lack of cholesterol leads to lipid barrier to break up and causes loss of skin moisture and protection against unwanted substances, such as chemicals. **Cholesteryl sulfate** (approximately 5 weight % of SC lipids) is an ester cholesterol and sulphuric acid and its function is probably to provide the SC cohesion.[10, 13, 19, 20]

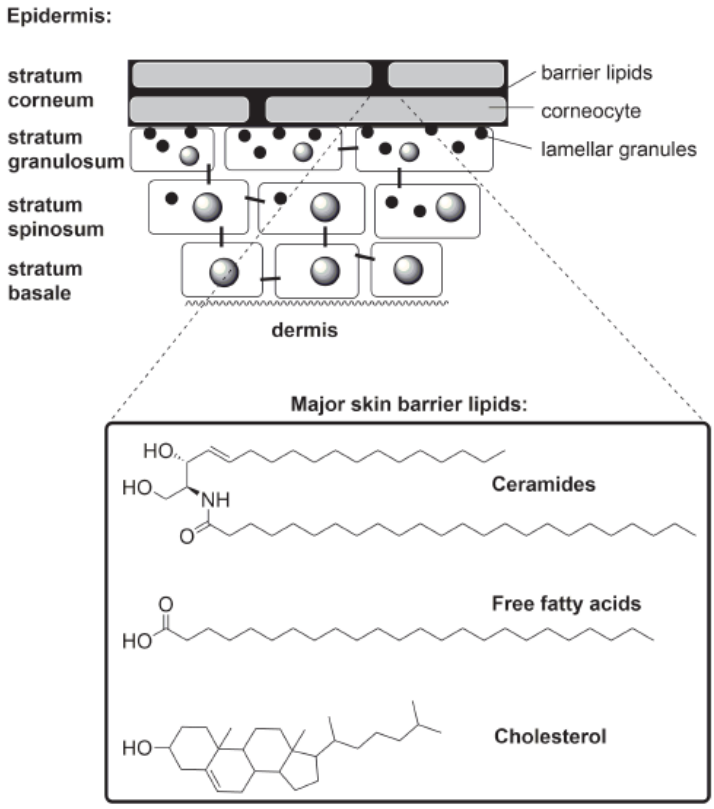

***Figure 3**. Structure of major skin barrier lipids in the SC lipid matrix, i.e., free fatty acids, cholesterol and ceramides.*[3]

1.3. Skin ceramides

Cer belong to large family of sphingolipids. Cer molecule consists of sphingoid base, which is normally 18 carbons,[17] and an acyl chain, which is unbranched and saturated, joined by an amide bond as shown in **Figure 4.** Cer form 40-50 % of lipids in SC; they protect

our body from water loss and from environmental factors such as dry air and pollution.[21] First part of Cer molecule comes from sphingoid base, such as **sphingosine**, **dihydrosphingosine**, **phytosphingosine**, and **6-hydroxysphingosine**.[22-25] (Dihydro)sphingosines are usually presented in eukaryotic cells, and their role is important in cell signalling.[26-28] The second carbon chain is derived from fatty acid. The acyl can be **non-substituted**, or **hydroxylated** in position **alfa-** or **omega-**. According to the acronyms of sphingoid bases ("S", "dS", "P", and "H" for sphingosine, dihydrosphingosine, phytosphingosine, and 6-hydroxysphingosine, respectively) and acronyms of acyl chains ("N" as non-substituted, "A" for alfa-hydroxylated and "O" for omega-hydroxylated acy), a useful skin Cer nomenclature was developed. This was for the first time published by Motta *et al*. in 1993.[21] The skin Cer are currently classified by this nomenclature.

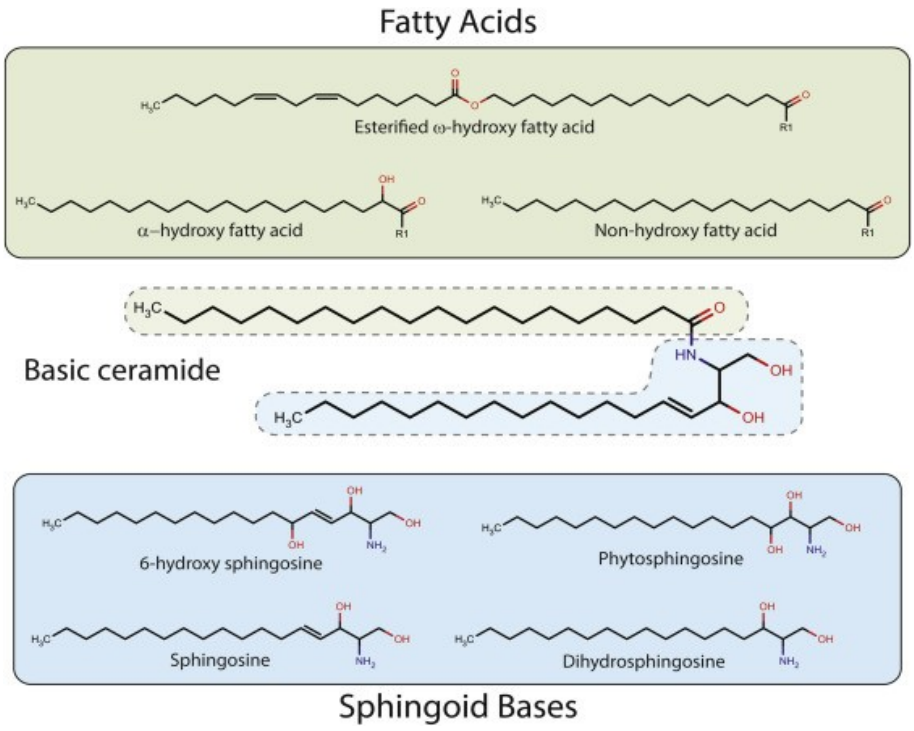

Figure 4*. Structure of skin ceramide and ceramide components, i.e., fatty acids and sphingoid bases (sphingosine, dihydrosphingosine, phytosphingosine, and 6-hydroxysphingosine).*[29]

According to the increasing age, the amount of Cer is reduced per time. This fact leads to dry and irritated skin and will lead to skin diseases, such as AD and psoriasis.[21, 30, 31] As the level of Cer in the outer layer of skin in patients with AD are reduced and there are variety of skin care products which contain Cer, which keeps the skin from being moist. [30]

1.4. Ceramide biosynthesis

The first reaction step in Cer biochemistry is the condensation of L-serine and palmitoyl-CoA catalysed by *serine palmitoyltransferase* (SPTLC1) in the presence of pyridoxal 5-phosphate, giving 18 carbon sphingoid base known as 3-ketosphingosine. SPTLC1 is a heteromeric protein, which is joined with long chain base biosynthesis protein 1 and 2 (LCBP1 and LCBP2) and *serine palmitoyl transferase* long chain base subunits (SPTLC1 and SPTLC2). The obtained product, 3-ketosphingosine is then metabolized by *NADPH-dependent-3-ketosphingosine reductase* (KDSR) giving rise to dihydrosphingosine. From dihydrosphingosine the dihydroceramide (catalysed by *ceramide synthase*) is formed.

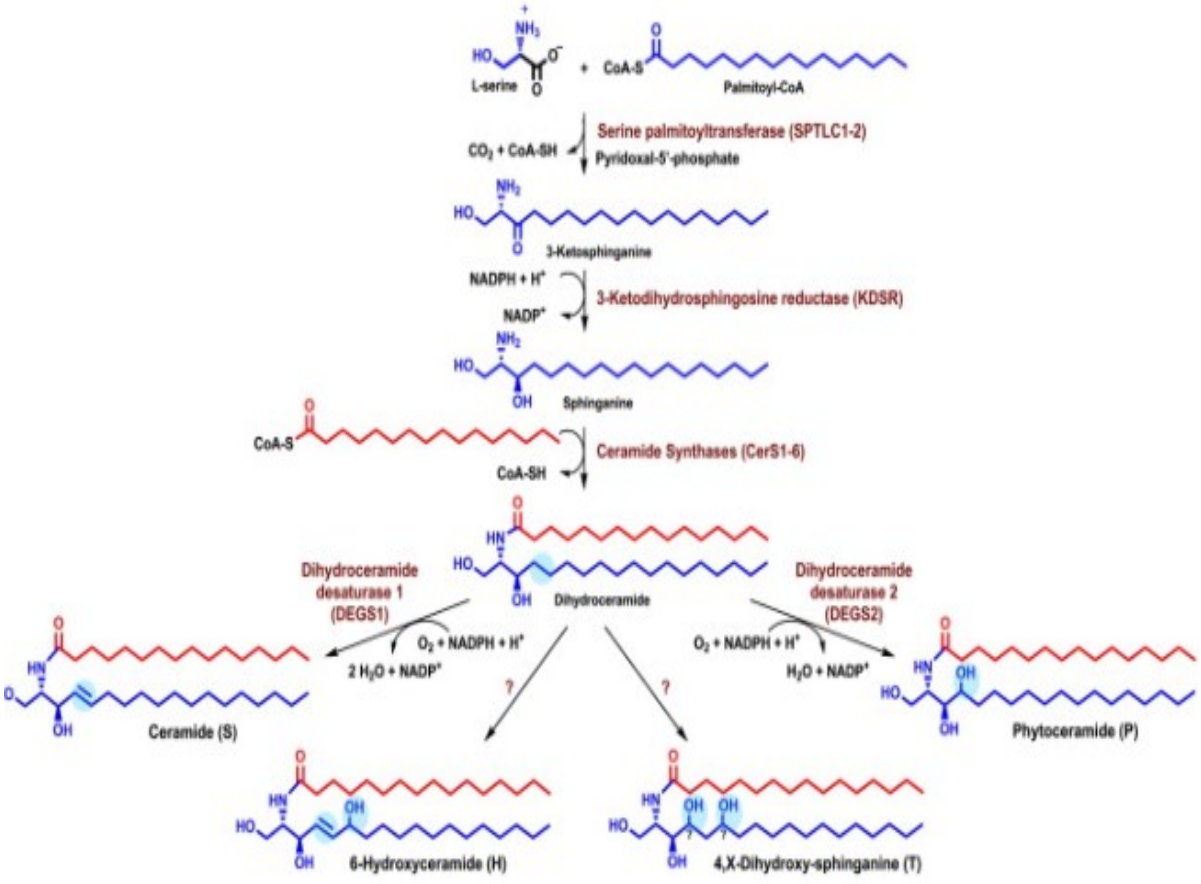

Figure.5*. Biosynthesis of skin Cer.*[32]

Dihydroceramide molecule is then metabolized to Cer by *dihydroceramide desaturase-1* (DEGS1), which needs oxygen and NAD(P)H as cofactors. Dihydroceramide is also

metabolized to phytoceramide (P) by the enzyme *dihydroceramide desaturase-2* (DEGS2). Furthermore, dihydroceramide is metabolized to 6-hydroxyceramide (H) and 4,X-dihydroxy-sphingosine (I) by unknown enzymes.[32, 33]

1.5. Organization of skin lipids in SC

The SC Cer consist of hydrophilic polar head, which is small (in contrast to phospholipids) and a long saturated chains in different conformation.[25] The Cer conformation in SC can be either **fully extended** (with the chain are leading to opposite direction) or **hairpin conformation**, in which long chains are leading the same direction as shown in **Figure 6**.

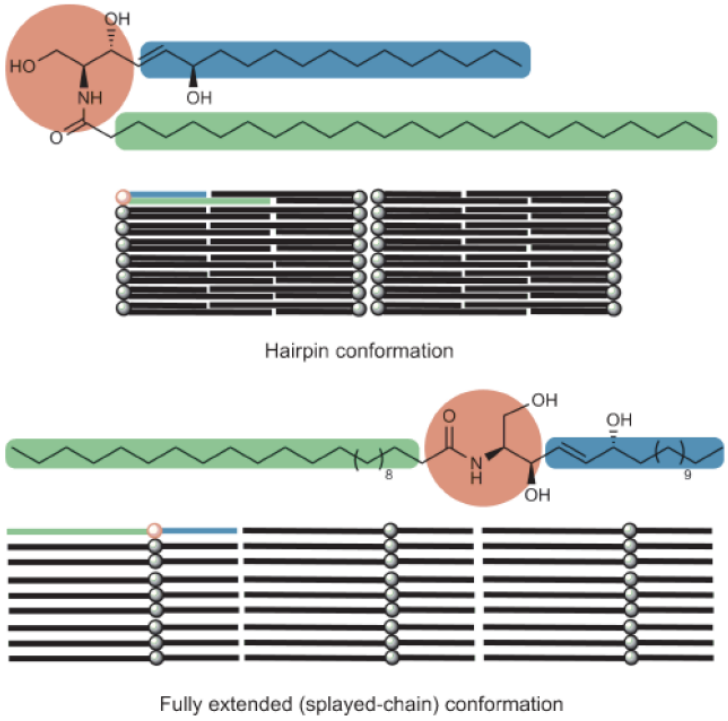

Figure 6. *Conformation of skin Cer in SC – hairpin, and full extended conformation.*[25]

In a healthy human skin, the lateral packing of the skin lipid can be **orthorhombic**, **hexagonal** and **liquid/fluid** (**Figure 7**). These three phases (organizations) are physiological and occur in the lipid matrix. Orthorhombic sub-cell is characterised for tight packed methylene chains with majority of all-*trans* conformers.[34-37] This orthorhombic sub-cell is necessary for the proper barrier function. Lower amounts of skin lipids are in **hexagonal** and

liquid (approximately 1%) sub-cell. In this lipid arrangement, methylene chains are in more mobile *gauche* conformation. [38]

Interestingly, the barrier function in patients with AD is reduced and it results in a hexagonal lateral packing, which have greater mobility in comparison to orthorhombic packing. They can also have liquid packing, which in fact has the greatest mobility.[39]

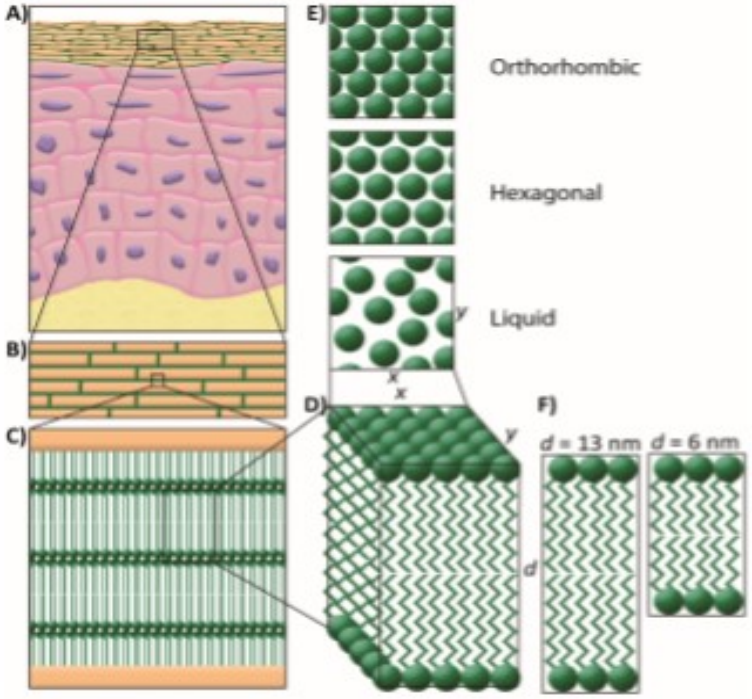

***Figure 7**. Stratum corneum (SC; panels A and B) and lipid lamellae (panel C), and its lamellar (panel D and F) and lateral organization (panel E).*[38]

1.6. Glucosyl ceramides

Glycosyl ceramides (GlcCer) consist of a Cer molecule and monosaccharide (glucose) or oligosaccharide. Saccharide unit is connected with OH- group (C1) of Cer. The main role of GlcCer is the reservoir function for Cer synthesis, they are the precursors of barrier Cer. GlcCer are converted to Cer by β-glucosyl cerebrosidase (GlcCer'ase; **Figure 8**). Production of Cer can be reduced due to changes in GlcCer'ase, which leads to impaired SC lipid lamellae and reduced barrier function. A typical example where diminished Cer have been found is in patients with Gaucher disease. There four times higher epidermal GlcCer/Cer ratio have been described. Additionally, GlcCer'ase requires initiation by saposins (sphingolipid activator

proteins). Patients with psoriasis vulgaris and AD have reduced amount of prosaposin which is a saposin precursor leading to a diminished Cer and GlcCer accumulation. [40]

Cer deficiency by hydrolysis of GlcCer, which is catalyzed by the enzyme glucosylceramide-β-glucosidase, disrupts the barrier function; this influences the epidermal water loss (TEWL) in patients with psoriasis. Studies show that patients with psoriasis (non-lessional skin) have lower mRNA expression of GlcCer'ase. However, the level of GlcCer'ase was higher in lessional psoriatic skin in comparison to non-lessional skin. Removal of saposin precursor pro-saposin which is required for activation of both GlcCer'ase and sphingomyelinase result in Cer deficiency and GlcCer accumulation. Patients with psoriasis vulgaris and AD have lower levels of prosaposin in comparison to healthy skin.[40]

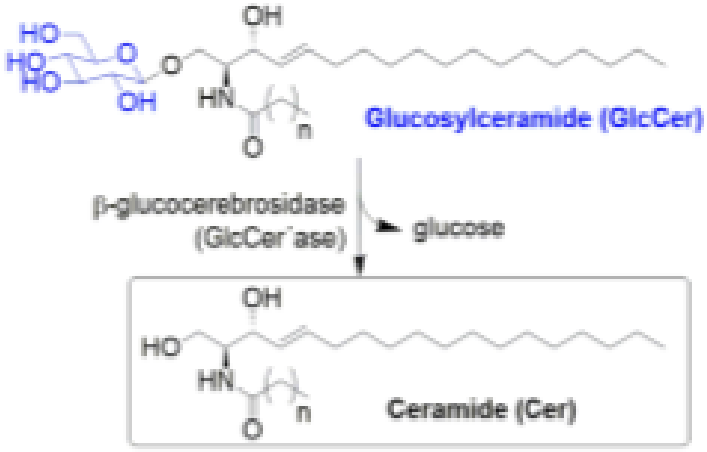

Figure 8*. Conversion of glucosyl ceramide (GlcCer) to ceramide (Cer) by β-Glucocerebrosidase.* [40]

1.7. Glucosyl sphingosine

Glucosyl sphingosines (GSP) belong to lysolipids (formed from Cer precursors by hydrolysis, see below) and are found in plasma membranes. They are involved in many functions including cell signalling, metastasis, cell differentiation, interaction between cell surfaces, cell adhesion, cell growth, oncogenesis and rises the level of calcium movement from intercellular stores.[41-43]

1.8. Role of Cer deficiency and GSP in patients with AD

Patients with AD have lower quantities of Cer in comparison to healthy skin. Instead of Cer, the skin of AD patients occurring high GSP levels that have low moisture content due to impaired barrier function of the SC. However, there has been no abnormality of the enzymes used in Cer biosynthesis such as *serine palmitoyl transferase* long chain base subunits (SPTLC1 and SPTLC2) or *ceramide synthase*. Furthermore, it has been demonstrated that the enzyme *glucosylceramide deacylase* removes the *N*-acyl linkage of the glucocerebroside (GlcCer) leading to formation of GSP (**Figure 9**) resulting in Cer deficiency in patients with AD.[41-43]

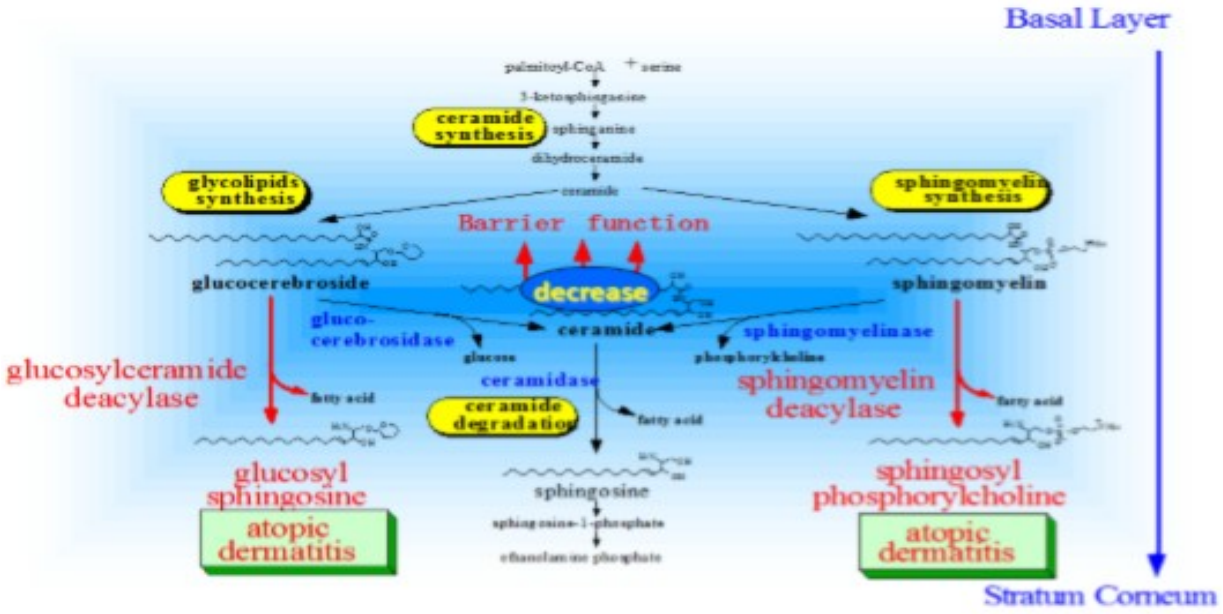

Figure 9*. Glycosyl sphingosine (GSP) formation pathway in atopic dermatitis (AD) patients.*[41]

1.9. Role of Cer deficiency and GSP in Gaucher disease

Gaucher disease (GD) is defined as an acceleration of glucocerebroside due to lack of the enzyme *glucocerebrosidase*. However, it has also been discovered that GSP can lead to GD as it inhibits the enzyme *glucocerebrosidase* as shown in **Figure 10.** GD patients have lower Cer (both free and protein-bound Cer species) in comparison to healthy skin as they have higher epidermal ratio of GlcCer/Cer and the lipids in the SC are loosely packed. Holleran *et al* [44] proposed that the persistence of GlcCer, rather than Cer deficiency is more probable to be the cause for the abnormalities of the membrane structural leading to the

skin lessions in type 2 GD, as topical Cer did not stop the harmful effects of the GlcCer'ase inhibitor 5. However, the inhibitor did not cause Cer deficiency. [45, 46]

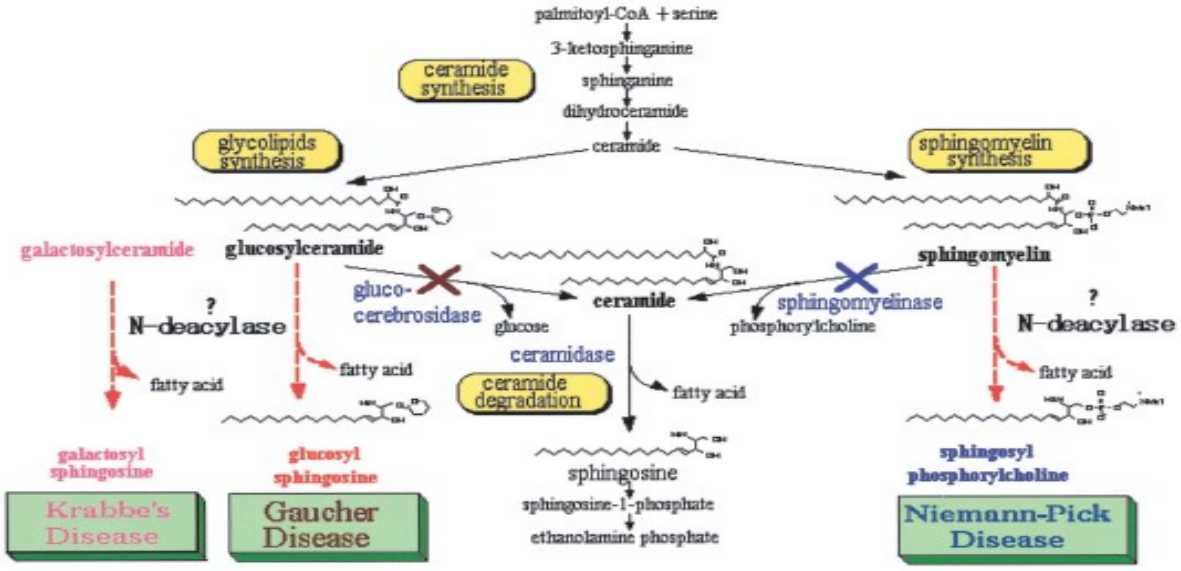

***Figure 10**. Sphingolipid metabolism discovered in GD.*[41]

Furthermore, it was also demonstrated that increased levels of GSP may lead to bone diseases such as osteopenia (a condition in which protein content of bone tissue is reduced) osteonecrosis (death of bone tissue), osteosclerosis (decrease in bone density and hardening of the bone). GSP decreases the bone density in GD patients by reducing the mesenchymal stem cells MSCs. GSP also reduces the level of calcium by osteoblast in GD patients. Researchers think that it might be due to reduction of osteoblasts from MSCs and also reduction of function.[45, 46]

2. Aim of the study

The aim of this study is to study the impact of an addition of Cer metabolite (lysolipid GSP) on the permeability of the isolated human SC. In this thesis, the permeability markers, such as trans-epidermal water loss (TEWL), electrical impedance, flux of theophylline (TH) and flux of indomethacin (IND) have been studied. The partial aim of the work was to prepare the SC models by using their isolation from the human skin (control samples). In addition, we aimed to prepare SC models with an addition of GSP. The SC model permeation experiment was performed in Franz diffusion cells. Afterwards, we aimed to investigate the role of GSP on the microstructure and lipid chain order of SC after the application of GSP. This parameter was studied by infrared spectroscopy.

3. Materials and methods

3.1. Chemicals and other materials

GSP was purchased from Avanti Polar Lipids (Alabaster, USA). Indomethacin (IND), theophylline (TH), gentamicin, propylene glycol (PG), ethanol (EtOH) and other solvents and (in)organic chemicals (for buffer preparation) and trypsin from porcine pancreas (1:250 powder, 1500 BAEE units/mg solid) were purchased from Merck Company (Schnelldorf, Germany). The aqueous solutions were prepared from Millipore water. The chemicals were analytical grade and used without further purification. All solvents were analytical or HPLC grade.

3.2. Isolation of human SC

The human skin was obtained from female patients who had undergone a plastic surgery in private hospital SANUS in Hradec Králové. The frozen skin was added into Millipore water at 60°C for 30 seconds. This is a key step for better epidermis removing. Afterwards, the epidermis was carefully removed from the dermis by tweezers and then was added into a physiological buffer (PBS solution, 10 mM buffer adjusted to 150 mM ionic strength containing 137 mM NaCl, 8 mM $Na_2HPO_4.12H_2O$, 2 mM $NaH_2PO_4.2H_2O$) at pH 7.4 with 0.5% trypsin (trypsin enzyme is essential for tearing down of epidermal „living“ layers, because only the SC was needed for the experiment) and let it at 32°C overnight. After that, the SC was washed with Millipore water and acetone (2-3 times). Acetone is an organic solvent which is used to remove the rest of surface lipids.[40, 47, 48]

3.3. Permeation experiment

After the washing the SC, the tissue fragments were cut into squares 2 cm × 2 cm. SC was then applied onto the supporting polycarbonate filters by tweezers and cotton swabs. After that, the samples (SC + supporting filters) were then mounted into Teflon holders with a diffusion area of 1.0 cm^2 and the holders were installed into Franz diffusion cells with an acceptor compartment volume of ± 6.5 mL; the exact volume for each cell were measured one by one and were involved in the calculation. The Franz cells were filled with a PBS buffer at pH

7.4 containing 50 mg/mL gentamicin as a preservative. The cells were then put into the water bath at physiological skin temperature of 32°C. After 12h equilibration, the electrical impedance and trans-epidermal water loss (TEWL) were measured (see below). After the measuring, 100 µL of 1% GSP solution in PG/EtOH 7:3 (v/v) or the mixture of solvents (control samples) were applied onto the SC samples, and the samples were equilibrated overnight.[40] After the washing of the rest of solvents/solution of 1% GSP, the electrical impedance and TEWL were measured once more. The next day, 100 µL of 2% of IND or 5% of TH suspensions in 60% PG were applied on the samples. Next, 300 µL of the PBS solutions from the Franz cells were taken every 2 hours for 8 hours and were substituted by PBS. The concentration of either TH or IND were measured by high performance liquid chromatography (HPLC, see below).[48]

3.4. High performance thin layer chromatography (HPTLC) analysis of sample lipids

High performance thin layer chromatography (HPTLC) according to Bleck *et al* [49] and Vávrová *et al* [50] with small modifications was used to evaluate qualitative and quantitative analysis of the isolated SC lipids. The samples were prepared in the same banner as in permeation experiment. The isolated SC + supporting filter was incorporated with Teflon holders into Franz diffusion cells. After 3h equilibration, the 1% solution of GSP (100 µL) was applied on the SC and equilibrated overnight. The Franz cells were removed from the water bath, SC in Teflon holders was washed with Millipore water and dried with ear cleaner. Afterwards, the SC was removed from the holders, left on the supporting filters, and washed again with Millipore water. From the samples the diffusion area was cut off; this area of tissue was washed, dried on gaze, placed into vials, then dried in desiccator overnight and storage in freezer. SC samples in vials (controls or SC with GPS) were first extracted in chloroform/methanol (2:1, v/v; approximately 1 mL) for 2 hours, organic solutions were filtrated, evaporated under stream of nitrogen and dried over phosphorous dioxide overnight.

The glass plate (silica gel 60, Merck, Darmstadt, Germany) was washed with 1:2 methanol (MeOH)-$CHCl_3$ (v/v). Then, dried and equilibrated for 30 min at 120°C in drying oven. The samples from tissue extraction were dissolved in in 1:2 MeOH-$CHCl_3$ (v/v) at concentration 200 µL/mg of SC. The samples were (under a stream of nitrogen) sprayed (injection volume of 30 µL) on an HPTLC glass plate by using Linomat 5 (Camag, Muttenz, Switzerland). Then, the

HPTLC plate was developer twice with 4.5:95:0.75 MeOH-$CHCl_3$-acetic acid (v/v/v) in a developing chamber (Camag, Muttenz, Switzerland). For the visualisation of spots (Scanner 3; Camag, Muttenz, Switzerland), an aqueous solution of 8% H_3PO_4 (v/v), 10% $CuSO_4$, 5% methanol was used, the HPTLC plate was immersed into this solution for 10 s and then dried in a drying oven for 30 min at 160°C. [48]

3.5. Trans-epidermal water loss (TEWL)

TEWL measures the water loss on the human skin. In this experiment, the water loss of SC samples was measured using AquaFlux (condenser chamber measurement method) AF 200 instrument (Biox Systems Ltd, UK) at 30–36% relative air humidity and 24–26 °C. According to this, the TEWL value is defined as the steady-state flux density of water diffusing through the SC sample.[40]

3.6. Electrical impedance

After measuring the TEWL, the electrical impedance was measured using an LCR meter 4080. Measuring range 20 Ω to 10 MΩ, with an alternating frequency of 120 Hz was used. The electrical impedance is the resistance of the SC tissue SC against the flux of ions. It is an explanation of the opposition of the electrical current, the resistivity of the skin is indirectly related to the permeability to polar chemicals or ions. It is also used to measure the skin quality. Before the measuring of electrical impedance, 500 µL of PBS (at pH 7.4) were added to each SC sample. After 1h of equilibration, the measurement was done by adding one electrode in the donor compartment and the other in the shoulder of acceptor compartment of the Franz cell. The measurement was done individually for each cell.[47, 48] The electric impedance was also measured in samples after the application of the solvents/ solution of 1% GSP.

3.7. Model permeants for permeation studies

As donor samples (*i.e.,* the model permeants), 2% (w/w) suspension of IND and 5% (w/w) suspension of TH were prepared from 60% PG (v/v). Before the experiment, suspensions were stored in thermostat at 32°C. Before the application, the suspensions were resuspended using shaking equipment.[51]

3.8. High performance liquid chromatography (HPLC) of model permeants

The concentrations of TH (IND) were measured using a Shimadzu Prominence instrument (Shimadzu, Kyoto, Japan), which consists of SPDM20A diode array detector, SIL-20A HT autosampler, LC-20AD pumps with a DGU-20A3 degasser and CBM-20A communication module. The TH and IND containing samples were measured by isocratic reverse-phase HPLC. Data were examined using the LC Solutions 1.22 software.

TH detection: The mixture of methanol and 0.1 M NaH_2PO_4 (4:6, v/v) was chosen as a mobile phase at a flow rate of 1.2 mL/min at 35°C. The reverse phase for a separation of TH was achieved on a LiChroCART 250-4 column. Acceptor sample (20 µL) was injected into the column, and the UV absorption was measured at 272nm, with a bandwidth of 4 nm. TH retention time was 3.2 ± 0.1 min.

IND detection: The mobile phase containing acetonitrile, water and acetic acid (90:60:5, v/v/v) at a flow rate of 2 mL/min was used. The IND samples were assayed on a LiChroCART 250-4 column (LiChrospher 100 RP-18, 5 µm, Merck). 100 µL of acceptor phase sample was injected into the column, which was maintained at 40°C. At a wavelength of 260 nm the UV absorption of IND peak was observed. The retention time of IND was 3.1 ± 0.1 min. [52]

3.9. Fourier-transform infrared spectroscopy (FTIR)

FTIR spectroscopy was used to evaluate the conformation of the lipid chains after the application of GSP on the SC. FTIR spectra were assembled on a Nicolet 6700 spectrometer with a single-reflection MIRacle ATR ZnSe crystal (PIKE technologies, Madison, WI). The spectra were initiated by the addition 256 scans collected at 2 cm^{-1} resolution. FTIR spectra was evaluated at a laboratory temperature. The spectra were examined by Bruker OPUS software. The second derivative evaluates the exact peak positions.[53]

3.10. Permeation data evaluation

The steady state flux of TH or IND [µg/cm^2/h] were calculated as a slope of the linear regression function obtained by fitting the linear region of the plot in Excel, the cumulative

amounts were plotted against the time. The number of replicates is given in the pertinent figure and the data are presented as the means ± standard error of mean (SEM). For the statistical analysis unpaired t-test (program GraphPad Prism) was used.

4. Results and discussion

In this diploma thesis, we aimed to investigate the role of one selected Cer-precursor metabolite on the barrier properties of human skin. In this work we studied the effect of GSP on the SC permeability and lipid chain order in the human skin tissue. First of all, we isolated the human epidermis from the female donor patients using validated method [54], *i.e.,* the immersion of the washed skin into the hot Millipore water. Then, the epidermis was added into a solution of enzyme trypsin in physiological buffer. This was a key step for the SC isolation. Afterwards, the SC was incorporated into Teflon holders and Franz diffusion cells. After equilibration process, we measured the TEWL [55] and electrical impedance [56], and then we applied 1% solution of GSP in solvent mixture based on PG/EtOH or the "empty" solvents (PG/EtOH, 7:3, v/v) only. Second, the TEWL and electrical impedance were measured again. In addition, the permeation experiments with two different model permeants were performed. In following subchapters, the discussed results obtained from our experiments are described.

4.1. High performance thin layer chromatography

In this study, the HPTLC technique was used with aim to detect and quantify the amounts of GSP and other skin lipids in control and samples with lysolipid. First, the samples were extracted into organic solvents and then quantified using Linomat 5 equipment. To quantify the skin lipid, the calibration (reference) solutions were prepared. According to these references, the Chol, FFA, main Cer subclasses (sphingosine-based Cer: NS, EOS, AS, phytosphingosine-based Cer: NP, AP, EOP) and GSP were detected. Note: most polar Cer (Cer NH, and Cer AH) were calibrated in order to Cer AS and AP). From the experiment we extracted the amount of each lipid class [µg] per 1 mg of extracted tissue (SC). From the amounts we calculated the molar GSP/Cer ratio (percentage) for the samples (100* GSP [mol]/GSP [mol] + Cer [mol]). We found out that the average molar ratio of GSP was 23.35%.

4.2. TEWL and electrical Impedance

First, we measured the TEWL (**Figure 10**), which is one of the most important dermatological characteristics. This parameter is common used in dermatology [57]and some biophysical studies (also in *Skin Barrier Research Group*) [55, 58] used. After the mounting of

Teflon holders with SC samples, we measured the TEWL. The values of TEWL are shown in **Figure 10A** (first panel). First, the TEWL was measured on each sample without any application of solvents/solution of GSP (black and blue bars). After this, either solvents or solution of GSP were applied on the SC samples and TEWL was measured (black-white and blue-white bars in **Figure10A**). We additionally used blank supporting filters (without any SC tissue) as a negative control. The blank filters do not play any barrier role, thus, they do not affect the SC permeability. TEWL of supporting filters presents the "maximum/minimum" values.

Before the application of either GPS or only the organic solvents, the TEWL values reached 16.13 ± 0.84 and 19.64 ± 2.35 g/m^2/h (black and blue bars respectively). After the application of GSP or a mixture of PG + EtOH, the TEWL significantly increased (*i.e.,* 35.86 ± 0.92 and 47.29 ± 2.45 g/m^2/h, black-white and blue-white bars). However, the addition of GSP did not significantly change the TEWL, indeed it is higher but comparable with the TEWL of SC with solvent application. In addition, the value of TEWL for the negative control (supporting filter) was 100.25 ± 1.26 g/m^2/h.

From the values from panel A we calculated the TEWL fold change, *i.e.,* the ratio of TEWL after and before the application of PG/EtOH or 1% GSP solution in PG/EtOH. The value for the TEWL of the controls (without GSP) was 2.26 ± 0.11 g/m^2/h, which was comparable with the TEWL value of the samples with and addition of lysolipid GSP (2.60 ± 0.20 g/m^2/h). From this parameter we can conclude that the presence of GSP do not drastically affect the permeability to water molecules. The TEWL fold change is shown in **Figure 11A** (second panel).

After measuring the TEWL, we measured the electrical impedance of control samples and the samples with GSP (**Figure 11B**). We also measured the blank filters as negative controls (grey bar in first panel in **Figure 11B**). The electrical impedance of these filters (0.69 ± 0.12 kΩ × cm^2) represents the minimum value. In general, the higher the electrical impedance the better the permeability. The values of electrical impedance before the application of solvents or the solution of GSP were very similar. After the addition of PG/EtOH and solution of lysolipid increased the electrical impedance, *i.e.,* 17.18 ± 0.19 kΩ × cm^2 (black-white bar) and 4.30 ± 0.20 kΩ × cm^2 (blue-white bar). From the values after and before the application of organic solvents/GSP solution, the fold changes (ratios) were calculated. The fold change (**Figure 11B**, second panel) for the electrical impedance of the controls was 0.38 ± 0.05 kΩ × cm^2. However, addition of GSP significantly decreases the electrical impedance

(0.07 ± 0.01 kΩ × cm^2). This fact correlates with the trend in higher TEWL of GSP samples and could suggest the negative effect of the lysolipid on the permeability of human SC to ions.[56]

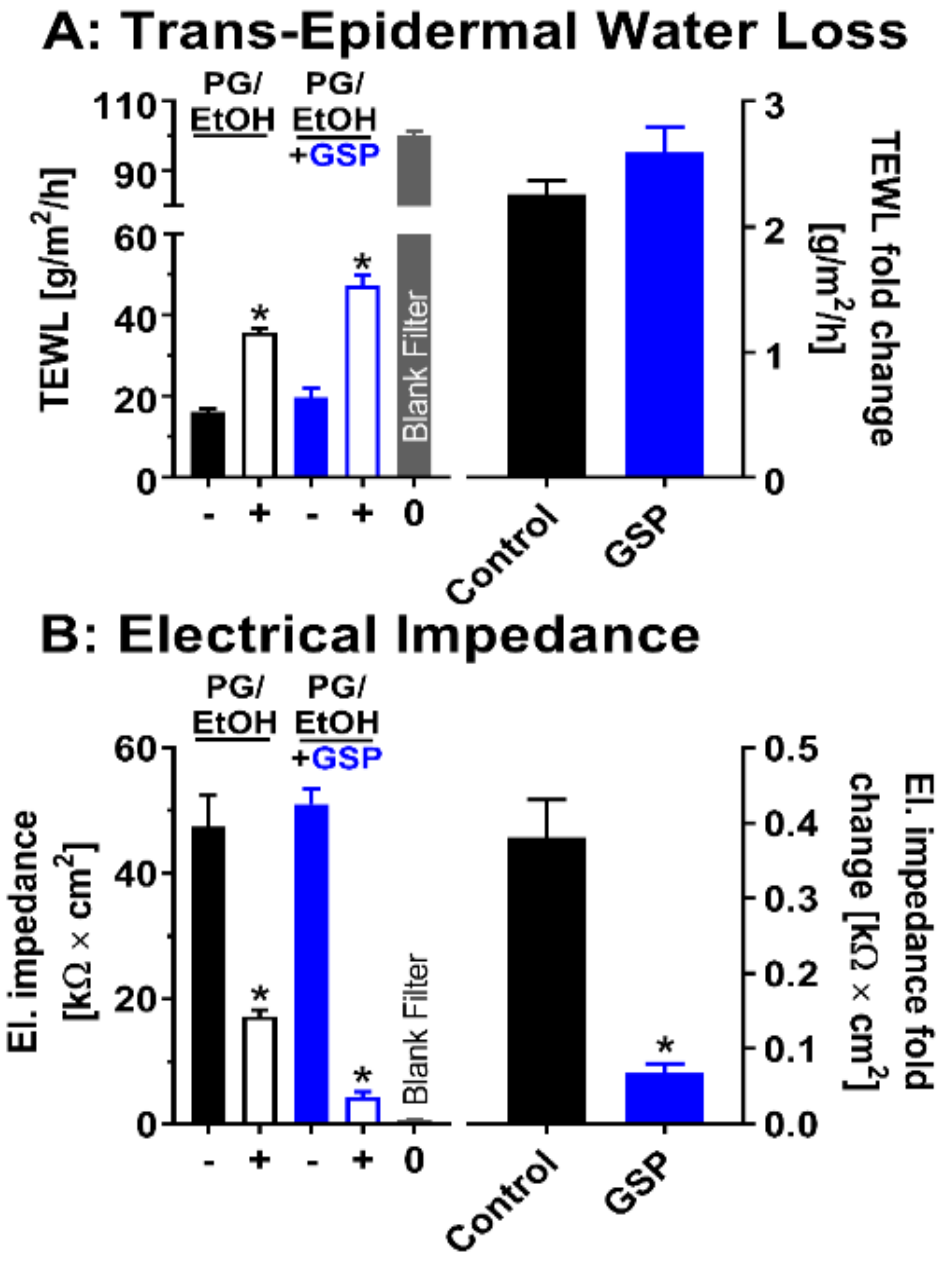

Figure 11*. Effect of GSP on the SC permeability. Water loss (A), electrical impedance (B), first panel in each graph represents the data before (minus mark, black and blue bars) and after the application of PG + EtOH/1% solution of GSP in PG + EtOH (plus mark, black-white and blue-white bars). The grey bars represent the values for blank supporting filters. Second graphs show the TEWL/electrical impedance fold change. Data are presented as the means ± standard*

*error of mean (SEM), (TEWL) n = 6-10, * statistically significant against controls. Note: PG, propylene glycol; EtOH, ethanol; GSP, glucosyl sphingosine.*

4.3. Permeability to theophylline (TH) and indomethacin (IND)

The model SC systems were studied in permeation experiments (**Figure 12**). In this work we selected two different model drugs. Note: the use of TH and IND was not because of their therapeutic effect but because of their physico-chemical properties.[59] TH is a small polar molecule with balanced lipophilicity (TH characteristics: M_w = 180,164 g/mol, logP = -0.02; IND characteristics: M_w = 357.79, logP = 4.27). After the electrical impedance measuring and the equilibration of Franz cells in water bath (32°C), we applied 100 µL of 5% TH suspension on each SC sample. After 2 h, we performed the sampling in following times: 2, 4, 6, and 8h. From the sampled solutions, the concentration using HPLC was determined, and using Excel program the cumulative amount (**Figure 12**, first panels) and flux of TH (and IND) were calculated.

The flux of TH (**Figure 12A**, second panel) for the control membrane (*i.e.,* the SC after the application of PG/EtOH) was 1.95 ± 1.96 µg/cm^2/h, while the permeability to TH of after the application of GSP on SC increased the flux to 3.75 ± 1.30 µg/cm^2/h. We can observe the negative effect of lysolipid addition, however this difference was not significant. We also measured the blank supporting filters (negative controls). These should logically represent the maximum value for the flux of TH. We calculated the flux of TH for the blank filters, which was 3269 ± 174.8 µg/cm^2/h.

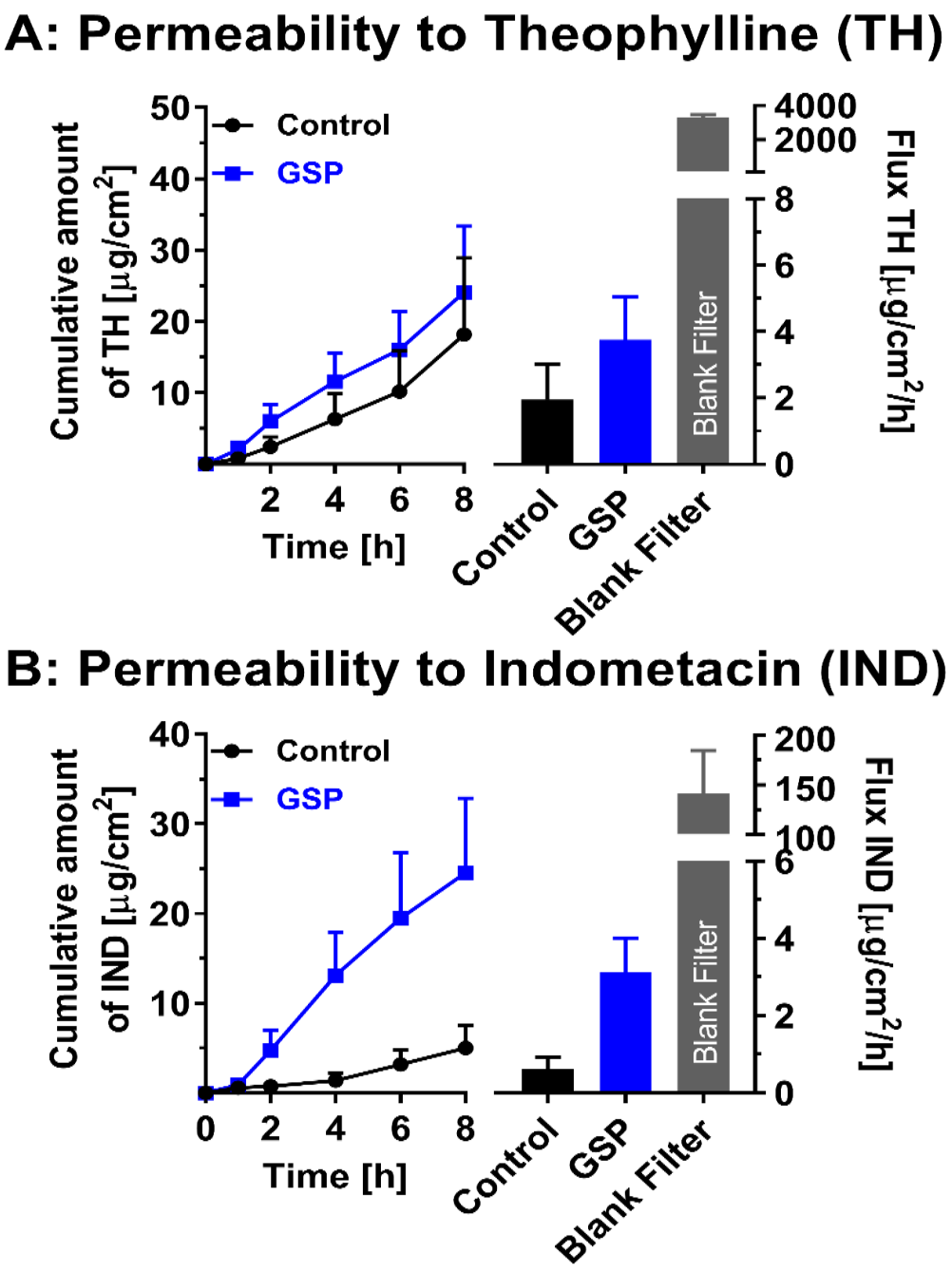

***Figure 12**. Effect of GSP on the SC permeability. Permeability to TH (A) and permeability to IND (B). First graphs in each panel represent the cumulative amounts of model permeant, second graphs show the flux of the compound. Data are presented as the means ± standard error of mean (SEM), n = 4-11.*

Similar results were observed in permeability of SC samples to IND (**Figure 12B**), the second model permeant that represents the compounds with large molecular weight and lipophilicity. From the concentrations measured by HPLC we calculated the flux of control

membrane, which was 0.61 ± 0.31 μg/cm^2/h. When the lysolipid (GSP in this case) is applied on the SC, the permeability to IND increased (flux of 3.14 ± 0.87 μg/cm^2/h, without statistical differences). The flux to IND for negative controls was 140.9 ± 43.66 μg/cm^2/h.

From the permeation studies we can conclude that the addition of GSP partially increases the permeability to water, small polar molecules and large lipophilic molecules. However, these changes are not significant. In contrast to TEWL, GSP samples are more permeable to ions (higher electrical impedance). This could suggest the change in SC integrity, lipid organization, etc. Therefore, we performed the biophysical studies (infrared spectroscopy, see below).

Similar trend in higher permeability of model SC membranes was observed in study published by Sochorová *et al.* [40] They aimed to investigate the role of Cer precursors, the GCer, *i.e.,* they studied the effect of GlcCer accumulation on the permeability of SC membranes. The samples were prepared in 1:1:1 molar ratio of isolated human Cer (hCer)/FFA/Chol, then isolated hCer were substituted by GlcCer. Substitution of 5–25% hCer by GlcCer led to higher permeability to small polar molecules (*i.e.,* to TH),[59] whereas in my experiment GSP increased the permeability to Th, however without statistical differences. Furthermore, the samples were further substituted by 50–100% of hCer by GlcCer which lead to lower permeability to small polar molecule (TH) than of the control. The permeabilities to IND and the TEWL with 5–25% GlcCer also increased. Furthermore, the model membrane systems with 5–25% GlcCer led to decreased value of electrical impedance over that of the control (statistically significant). This article is closely related to GSP, as GSP is formed from GlcCer by the enzyme *glucosylceramide deacylase*.[41] From this we can hypothesize that both the precursors of Cer (GCer) and their metabolites (GSP) do not lead to maintain the barrier properties.

4.4. FTIR spectroscopy

The second part of this study was to investigate the effect of lysolipid GSP on the SC microstructure, the chain order of lipids in lipid matrix of SC.[20, 40, 53, 60-62] We used the isolated SC, prepared according to the described procedure above. The isolated SC in vials was added into mixture of solvents (PG/EtOH) or into a solution of GSP (1% concentration). The SC without any application of solutions have been also prepared. Three types of samples were

measured using ATR-FTIR spectroscopy. In this case we observed the methylene symmetric stretching, the very sensitive vibration to lipid chain order. In healthy human skin, barrier lipids are well ordered (a presence of all-*trans* conformers), which is characterized by the wavenumber under 2850 cm^{-1}. In all the studied samples, the poly-methylene lipid chains are well ordered.[63, 64] The chain order of our samples is in following order: SC control samples (2848.59 ± 0.12 cm^{-1}) < SC + PG/EtOH (2849.13 ± 0.27cm^{-1}) < SC + 1% GSP solution (2849.39 ± 0.1 cm^{-1}). The wavenumbers are shown in **Figure 13A**. From this experiment we can conclude that the addition of lysolipid increases apparently chain disorder, however the differences between the values are not mathematically significant. The representative FTIR spectra of methylene symmetric stretching are shown in **Figure 13B**.

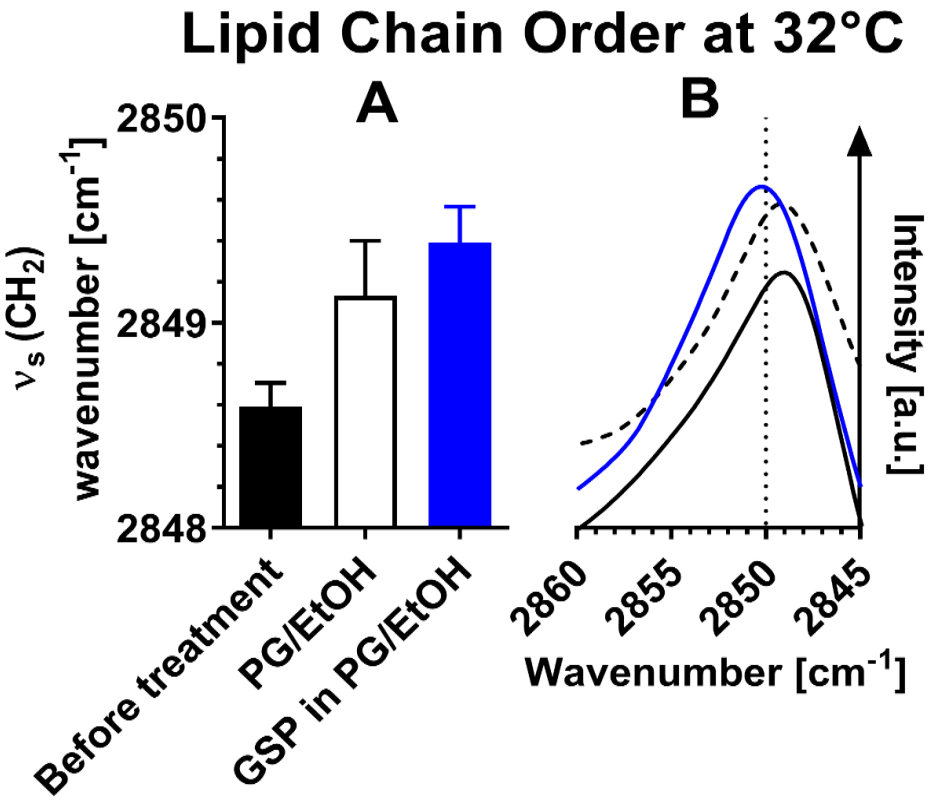

Figure 13*. Effect of GSP on the lipid chain (FTIR spectroscopy). Panel A shows the wavenumbers of symmetric stretching at physiological temperature of 32°C and panel B depicts the representative spectra. Data are presented as the means ± standard error of mean (SEM), n = 4. Note: PG, propylene glycol; EtOH, ethanol; GSP, glucosyl sphingosine.*

5. Conclusion

The goal of this work was to describe the behaviour of lysolipids in human SC. This work comes from other works, where the role of lysolipids (glucosyl sphingosine and sphingosine phosphorylcholine) has been investigated in model SC lipid membranes.

In this study, we isolated human skin tissue, the SC from female patients. First, we had to isolate the epidermis and SC. Then, the lysolipid GSP was applied onto the SC. Afterwards we performed the permeation experiments. From these results we can conclude that the GSP has partially detrimental effects on the SC permeability. We observed the trend in higher permeability in following permeation markers, *i.e.,* higher values of TEWL, permeability to polar molecules and lipophilic compounds. In addition, the GSP significantly decreases the SC resistance (electrical impedance), after its application on the SC. These results correlate with the experiments performed with other lysolipid (sphingosine phosphorylcholine), however these results belong to another diploma thesis.

To confirm the negative effect of GSP we studied the lipid chain order using infrared spectroscopy. From FTIR spectra we found out that the methylene chains are well but less ordered than those in SC without the high amounts of GSP. This work supports the results from other studies. The general aim of this study was to understand the role of lysolipids in healthy and diseased skin. The results will be helpful to for better understanding the human skin pathophysiology*, e.g.,* atopic dermatitis or Gaucher disease.

6. Abbreviations

AD	atopic dermatitis
AF	Aqua flux
ATR-FTIR	attenuated total reflection Fourier-transform infrared spectroscopy
Cer	ceramide
Chol	cholesterol
CerNS	N-tetraacosanoyl-D-erythro-sphingosine
DEGS1	dihydroceramide desaturase-1
DEGS2	dihydroceramide desaturase-2
EtOH	ethanol
FFA	free fatty acid(s)
FTIR	Fourier-transform infrared spectroscopy
GlcCer	Glycosylceramides
GlcCer'ase	β-glucoscerebrosidase
GD	Gaucher disease
GSP	glucosyl sphingosine
HPLC	high-performance liquid chromatography
IND	indomethacin

KDSR	ketosphingosine reductase
MSCs	mesenchymal stem cells
Mw	molecular weight
NADPH	nicotinamide adenine dinucleotide phosphate hydrogen
PBS	physiological buffer solution
PG	propylene glycol
SC	stratum corneum
SEM	standard error of mean
SC	sphingomyelin
SPC	sphingosine phosphorylcholine
SPTLC1	serine palmitoyltransferase long chain-1
SPTLC2	serine palmitoyltransferase long chain-2
TH	theophylline
TEWL	trans-epidermal water loss

7. List of figures

8. References

1. Hou, S.Y., et al., *Membrane structures in normal and essential fatty acid-deficient stratum corneum: characterization by ruthenium tetroxide staining and x-ray diffraction.* J. Invest. Dermatol., 1991. **96**(2): p. 215-23.
2. Wertz, P.W., *Lipids and barrier function of the skin.* Acta Derm. Venereol. Suppl. (Stockh), 2000. **208**: p. 7-11.
3. Vávrová, K., A. Kováčik, and L. Opálka, *Ceramides in the skin barrier.* 2017. **64**(2): p. 28.
4. Grabowski, S.R. and G.J. Tortora, *Principles of anatomy and physiology*. 2000: Wiley.
5. Williams, A., *Transdermal and dermal drug delivery: From theory to clinical practice*. 2003, London, Pharmaceutical Press. ISBN 0-85369-489-3.
6. (e-book), A.a.P., *https://opentextbc.ca/anatomyandphysiology/chapter/5-1-layers-of-the-skin/ (online).*
7. Eucerin.cz, *Struktura a funkce kůže.* http://www.eucerin.cz/o-kuzi/zakladni-informace/struktura-a-funkce-kuze (online).
8. Candi, E., R. Schmidt, and G. Melino, Nat. Rev. Mol. Cell Biol., 2005. **6**: p. 328.
9. Lampe, M.A., et al., *Human stratum corneum lipids: characterization and regional variations.* J. Lipid Res., 1983. **24**(2): p. 120-30.
10. Mojumdar, E.H., G.S. Gooris, and J.A. Bouwstra, *Phase behavior of skin lipid mixtures: the effect of cholesterol on lipid organization.* Soft Matter, 2015. **11**(21): p. 4326-4336.
11. White, S.H., D. Mirejovsky, and G.I. King, *Structure of lamellar lipid domains and corneocyte envelopes of murine stratum corneum. An X-ray diffraction study.* Biochemistry, 1988. **27**(10): p. 3725-32.
12. Swartzendruber, D.C., *Studies of epidermal lipids using electron microscopy.* Semin Dermatol, 1992. **11**(2): p. 157-61.
13. Mojumdar, E., et al., *Stratum corneum lipid matrix: location of acyl ceramide and cholesterol in the unit cell of the long periodicity phase.* Biochimica et Biophysica Acta (BBA)-Biomembranes, 2016. **1858**(8): p. 1926-1934.
14. Craven, B., *Pseudosymmetry in cholesterol monohydrate.* Acta Crystallogr. Sect. B, 1979. **35**(5): p. 1123-1128.

15. Imokawa, G. and K. Ishida, *Role of ceramide in the barrier function of the stratum corneum, implications for the pathogenesis of atopic dermatitis.* J Clin Exp Dermatol Res, 2014. **5**(01): p. 1-12.
16. Shapiro, D. and H.M. Flowers, *Studies on Sphingolipids. VII. Synthesis and Configuration of Natural Sphingomyelins.* J. Am. Chem. Soc., 1962. **84**(6): p. 1047-1050.
17. Groen, D., G.S. Gooris, and J.A. Bouwstra, *Model membranes prepared with ceramide EOS, cholesterol and free fatty acids form a unique lamellar phase.* Langmuir, 2010. **26**(6): p. 4168-75.
18. Bouwstra, J.A., et al., *Structural investigations of human stratum corneum by small-angle X-ray scattering.* J. Invest. Dermatol., 1991. **97**(6): p. 1005-12.
19. de Jager, M.W., et al., *The phase behaviour of skin lipid mixtures based on synthetic ceramides.* Chem. Phys. Lipids, 2003. **124**(2): p. 123-134.
20. de Sousa Neto, D., G. Gooris, and J. Bouwstra, *Effect of the omega-acylceramides on the lipid organization of stratum corneum model membranes evaluated by X-ray diffraction and FTIR studies (Part I).* Chem. Phys. Lipids, 2011. **164**(3): p. 184-95.
21. Motta, S., et al., *Ceramide composition of the psoriatic scale.* Biochim. Biophys. Acta, 1993. **1182**(2): p. 147-51.
22. Stewart, M.E. and D.T. Downing, *A new 6-hydroxy-4-sphingenine-containing ceramide in human skin.* J. Lipid Res., 1999. **40**(8): p. 1434-9.
23. Robson, K.J., et al., *6-Hydroxy-4-sphingenine in human epidermal ceramides.* J. Lipid Res., 1994. **35**(11): p. 2060-8.
24. Stewart, M.E. and D.T. Downing, *Free sphingosines of human skin include 6-hydroxysphingosine and unusually long-chain dihydrosphingosines.* J. Invest. Dermatol., 1995. **105**(4): p. 613-8.
25. Kovacik, A., J. Roh, and K. Vavrova, *The chemistry and biology of 6-hydroxyceramide, the youngest member of the human sphingolipid family.* ChemBioChem., 2014. **15**(11): p. 1555-62.
26. Futerman, A.H. and Y.A. Hannun, *The complex life of simple sphingolipids.* EMBO Rep, 2004. **5**(8): p. 777-82.
27. Bartke, N. and Y.A. Hannun, *Bioactive sphingolipids: metabolism and function.* J. Lipid. Res., 2009. **50 Suppl**: p. S91-6.

28. Hannun, Y.A. and L.M. Obeid, *Principles of bioactive lipid signalling: lessons from sphingolipids.* Nat Rev Mol Cell Biol, 2008. **9**(2): p. 139-50.
29. Meckfessel, M.H. and S. Brandt, *The structure, function, and importance of ceramides in skin and their use as therapeutic agents in skin-care products.* Journal of the American Academy of Dermatology, 2014. **71**(1): p. 177-184.
30. Janssens, M., et al., *Lamellar lipid organization and ceramide composition in the stratum corneum of patients with atopic eczema.* J Invest Dermatol, 2011. **131**(10): p. 2136-8.
31. Macheleidt, O., H.W. Kaiser, and K. Sandhoff, *Deficiency of epidermal protein-bound omega-hydroxyceramides in atopic dermatitis.* J. Invest. Dermatol., 2002. **119**(1): p. 166-73.
32. Rabionet, M., K. Gorgas, and R. Sandhoff, *Ceramide synthesis in the epidermis.* Biochim. Biophys. Acta, 2014. **1841**(3): p. 422-434.
33. Mizutani, Y., et al., *Ceramide biosynthesis in keratinocyte and its role in skin function.* Biochimie, 2009. **91**(6): p. 784-90.
34. Norlen, L., *Skin barrier structure and function: the single gel phase model.* J. Invest. Dermatol., 2001. **117**(4): p. 830-6.
35. Bouwstra, J.A., et al., *Phase behavior of lipid mixtures based on human ceramides: coexistence of crystalline and liquid phases.* J. Lipid Res., 2001. **42**(11): p. 1759-70.
36. Damien, F. and M. Boncheva, *The extent of orthorhombic lipid phases in the stratum corneum determines the barrier efficiency of human skin in vivo.* J. Invest. Dermatol., 2010. **130**(2): p. 611-4.
37. Mendelsohn, R., C.R. Flach, and D.J. Moore, *Determination of molecular conformation and permeation in skin via IR spectroscopy, microscopy, and imaging.* Biochim. Biophys. Acta, 2006. **1758**(7): p. 923-33.
38. Berkers, T., et al., *Degree of skin barrier disruption affects lipid organization in regenerated stratum corneum.* Acta dermato-venereologica, 2018. **98**(3-4): p. 421-427.
39. van Smeden, J., et al., *The important role of stratum corneum lipids for the cutaneous barrier function.* Biochim. Biophys. Acta, 2014. **1841**(3): p. 295-313.
40. Sochorová, M., et al., *Permeability Barrier and Microstructure of Skin Lipid Membrane Models of Impaired Glucosylceramide Processing.* Sci. Rep., 2017. **7**(1): p. 6470.

41. Ishibashi, M., et al., *Abnormal expression of the novel epidermal enzyme, glucosylceramide deacylase, and the accumulation of its enzymatic reaction product, glucosylsphingosine, in the skin of patients with atopic dermatitis.* Laboratory investigation, 2003. **83**(3): p. 397.

42. Higuchi, K., et al., *The skin of atopic dermatitis patients contains a novel enzyme, glucosylceramide sphingomyelin deacylase, which cleaves the N-acyl linkage of sphingomyelin and glucosylceramide.* Biochemical Journal, 2000. **350**(3): p. 747-756.

43. Imokawa, G., *A possible mechanism underlying the ceramide deficiency in atopic dermatitis: expression of a deacylase enzyme that cleaves the N-acyl linkage of sphingomyelin and glucosylceramide.* Journal of dermatological science, 2009. **55**(1): p. 1-9.

44. Holleran, W.M., Y. Takagi, and Y. Uchida, *Epidermal sphingolipids: metabolism, function, and roles in skin disorders.* FEBS Lett., 2006. **580**(23): p. 5456-66.

45. Rolfs, A., et al., *Glucosylsphingosine is a highly sensitive and specific biomarker for primary diagnostic and follow-up monitoring in Gaucher disease in a non-Jewish, Caucasian cohort of Gaucher disease patients.* PloS one, 2013. **8**(11): p. e79732.

46. Weiss, K., et al., *The clinical management of type 2 Gaucher disease.* Molecular genetics and metabolism, 2015. **114**(2): p. 110-122.

47. Sochorová, M., et al., *Permeability and microstructure of cholesterol-depleted skin lipid membranes and human stratum corneum.* J Colloid Interface Sci, 2019. **535**: p. 227-238.

48. Pullmannová, P., et al., *Effects of sphingomyelin/ceramide ratio on the permeability and microstructure of model stratum corneum lipid membranes.* Biochim. Biophys. Acta, 2014. **1838**(8): p. 2115-26.

49. Bleck, O., et al., J. Invest. Dermatol., 1999. **113**: p. 894.

50. Vavrova, K., et al., *Filaggrin Deficiency Leads to Impaired Lipid Profile and Altered Acidification Pathways in a 3D Skin Construct.* J Invest Dermatol, 2014. **134**(3): p. 746-53.

51. Kováčik, A., et al., *Effects of 6-Hydroxyceramides on the Thermotropic Phase Behavior and Permeability of Model Skin Lipid Membranes.* Langmuir, 2017. **33**(11): p. 2890-2899.

52. Skolova, B., et al., *Phytosphingosine, sphingosine and dihydrosphingosine ceramides in model skin lipid membranes: permeability and biophysics.* BBA - Biomembranes, 2017. **1859**(5): p. 824-834.

53. Skolova, B., et al., *Different phase behavior and packing of ceramides with long (C16) and very long (C24) acyls in model membranes: infrared spectroscopy using deuterated lipids.* J. Phys. Chem. B, 2014. **118**(35): p. 10460-70.

54. KLIGMAN, A.M. and E. CHRISTOPHERS, *Preparation of isolated sheets of human stratum corneum.* Archives of Dermatology, 1963. **88**(6): p. 702-705.

55. Kopečná, M., et al., *Dodecyl Amino Glucoside Enhances Transdermal and Topical Drug Delivery via Reversible Interaction with Skin Barrier Lipids.* Pharmaceutical Research, 2017. **34**(3): p. 640-653.

56. Fasano, W.J. and P.M. Hinderliter, *The Tinsley LCR Databridge Model 6401 and electrical impedance measurements to evaluate skin integrity in vitro.* Toxicol. In Vitro, 2004. **18**(5): p. 725-9.

57. Netzlaff, F., et al., *TEWL measurements as a routine method for evaluating the integrity of epidermis sheets in static Franz type diffusion cells in vitro. Limitations shown by transport data testing.* Eur. J. Pharm. Biopharm., 2006. **63**(1): p. 44-50.

58. Stahlberg, S., et al., *Influence of a Novel Dimeric Ceramide Molecule on the Nanostructure and Thermotropic Phase Behavior of a Stratum Corneum Model Mixture.* Langmuir, 2017. **33**(36): p. 9211-9221.

59. Mitragotri, S., *Modeling skin permeability to hydrophilic and hydrophobic solutes based on four permeation pathways.* J. Control. Release, 2003. **86**(1): p. 69-92.

60. Mendelsohn, R., et al., *Kinetic evidence suggests spinodal phase separation in stratum corneum models by IR spectroscopy.* J Phys Chem B, 2014. **118**(16): p. 4378-87.

61. Moore, D.J., M.E. Rerek, and R. Mendelsohn, *Lipid domains and orthorhombic phases in model stratum corneum: evidence from Fourier transform infrared spectroscopy studies.* Biochem. Biophys. Res. Commun., 1997. **231**(3): p. 797-801.

62. Moore, D.J. and M.E. Rerek, *Insights into the molecular organization of lipids in the skin barrier from infrared spectroscopy studies of stratum corneum lipid models.* Acta Derm. Venereol. Suppl. (Stockh), 2000. **208**: p. 16-22.

63. Mendelsohn, R. and D.J. Moore, *Vibrational spectroscopic studies of lipid domains in biomembranes and model systems.* Chem. Phys. Lipids, 1998. **96**(1-2): p. 141-57.

64. Garidel, P., et al., *The microstructure of the stratum corneum lipid barrier: Mid-infrared spectroscopic studies of hydrated ceramide:palmitic acid:cholesterol model systems.* Biophysical Chemistry, 2010. **150**(1–3): p. 144-156.